Published in final edited form as:
Cell Cycle. 2009 December 15; 8(24): 4091–4102.

C. elegans mitotic cyclins have distinct as well as overlapping functions in chromosome segregation

Monique van der Voet[1,†], **Monique A. Lorson**[2,†,‡], **Dayalan G. Srinivasan**[2,§], **Karen L. Bennett**[3], and **Sander van den Heuvel**[1,2,*]

[1]Developmental Biology, Utrecht University, Utrecht, The Netherlands [2]The Massachusetts General Hospital Cancer Research Center and Harvard Medical School, Charlestown, MA USA [3]Department of Molecular Microbiology and Immunology, University of Missouri, Columbia, MO USA [§]Department of Ecology and Evolutionary Biology, Princeton, NJ USA

Abstract

Mitotic cyclins in association with the Cdk1 protein kinase regulate progression through mitosis in all eukaryotes. Here, we address to what extent mitotic cyclins in the nematode *Caenorhabditis elegans* provide overlapping functions or distinct biological activities. *C. elegans* expresses a single A-type cyclin (CYA-1), three typical B-type cyclins (CYB-1, CYB-2.1 and CYB-2.2), and one B3-subfamily member (CYB-3). While we observed clear redundancies between the *cyb* genes, *cyb-1* and *cyb-3* also contribute specific essential functions in meiosis and mitosis. CYB-1 and CYB-3 show similar temporal and spatial expression, both cyclins localize prominently to the nucleus, and both associate with CDK-1 and display histone H1 kinase activity in vitro. We demonstrate that inhibition of *cyb-1* by RNAi interferes with chromosome congression and causes aneuploidy. In contrast, *cyb-3(RNAi)* embryos fail to initiate sister chromatid separation. Inhibition of both cyclins simultaneously results in a much earlier and more dramatic arrest. However, only the combination of *cyb-1, cyb-3* and *cyb-2.1/cyb-2.2* RNAi fully resembles *cdk-1* inhibition. This combination of redundant and specific phenotypes supports that in vivo phosphorylation of certain Cdk targets can be achieved by multiple Cdk1/cyclin complexes, while phosphorylation of other targets requires a unique Cdk1/cyclin combination.

Keywords

C. elegans; cyclin B1; cyclin B3; mitosis; meiosis; cell cycle; chromosome congression; chromosome segregation

Introduction

Cyclin-dependent kinases (CDKs) and their associated cyclin regulatory subunits control progression through the eukaryotic cell-division cycle (reviewed in refs. 1 and 2). Activation of the CDK1 kinase triggers entry into mitosis, while CDK1 inactivation is required for mitotic exit. Expression, association and degradation of the cyclin subunits are critical in the regulation of CDK activity.

*Correspondence to: Sander van den Heuvel; S.J.L.vandenHeuvel@uu.nl.
†These authors contributed equally to this work.
‡Current addresses: Bond Life Sciences Center; University of Missouri; Columbia, MO USA;

All eukaryotes express a number of different cyclins. The members of this protein family share similarity predominantly within the "cyclin box", a conserved domain that mediates binding and activation of CDKs. "G_1 cyclins", "S phase cyclins" and "mitotic cyclins" have been defined by their pattern of expression, Cdk activation and cell cycle function. In addition, cyclin subfamilies (e.g., A or B-type) have been distinguished based on sequence similarity. These classifications are partly overlapping, as members of each subfamily share cognate CDK partners and show similar patterns of expression and associated kinase activity. Hence, the paradigm in the field has long been that specific CDK/cyclin combinations phosphorylate specific target proteins and thereby promote distinct cell cycle transitions. In metazoans, D-type cyclins together with Cdk4/Cdk6 promote progression through G_1 phase; E-type cyclins in association with Cdk2 support the onset of S phase; A-type cyclins in complex with either Cdk2 or Cdk1 act in the S, G_2 and M phases, and B-type cyclins together with Cdk1 control progression through mitosis.[3]

Cyclins expressed in the same cell cycle phase are largely redundant in function. Four different B-type cyclins (CLB1, CLB2, CLB3 and CLB4) regulate the progression through mitosis in budding yeast. However, expression of CLB2 alone is sufficient and *GAL1* driven expression of CLB1 complements the *clb1,2,3,4* deletion.[4,5] Three different cyclins, a single A-type and B-type cyclin and a member of the distinct B3 subfamily, cooperate during mitosis in Drosophila. Mutation of *Dm* CycB or CycB3 does not interfere with viability.[6] Furthermore, knockout of individual cyclins in mice result in limited defects, with the exception of cyclins A2 and B1.[7,8] The specific developmental defects associated with cyclin D1, cyclin D2 and cyclin D3 knockout appear to result from distinct patterns of expression of these cyclins, rather than specific functions.[9–12] In support of this idea, replacement of the cyclin D1 coding sequences with cyclin D2 rescues the cyclin D1 knockout phenotype.[13,14] CDK knockout experiments have shown that substantial mouse development is possible with Cdk1 alone, functioning in combination with a broad range of cyclins.[15] Such results are surprising, as specific functional properties would be expected to underlie the conservation of distinct cyclin subfamilies throughout metazoan evolution.

Indeed, a recent analysis indicates that Drosophila mitotic cyclin A, B and B3 cyclins are less redundant than previously concluded, as all three of these cyclins have specific critical functions in the syncytial embryo.[6,16] In fact, ample experimental evidence supports that cyclins contribute to the substrate specificity of CDKs and that members of different subfamilies cannot simply substitute for each other. Factors that contribute to cyclin specificity are subcellular localization,[17] and the use of a hydrophobic cyclin patch in substrate contact.[18,19] Thus far, the cyclin-substrate specificity is best characterized for budding yeast CLB5 and mammalian cyclin A.[18,19] For example, knock-in of *CLB2* into the *CLB5* locus in yeast prematurely initiates CLB2/CDC28 kinase activity and allows rescue of *clb1,2* lethality, but does not replace the role of *CLB5* in S phase initiation.[20] Phosphorylation of pRb, p107 and E2F-1 by Cdk2/cyclin A involves binding of the cyclin A hydrophobic patch to these substrates.[18] This explains why Cdk2 in association with cyclin A (but not cyclin B1) phosphorylates these substrates in vitro.[21] Other cyclins may also recruit specific targets through a distinct docking site or, alternatively, promote CDK activity towards a broader range of targets. For most cyclins it remains poorly understood if and how they confer target specificity to their CDK partners, which targets they recruit and which functions they share with other cyclins.

In the present study, we address to what extent mitotic cyclins have redundant versus specific functions in early *Caenorhabditis elegans* development. *C. elegans* embryos are particularly amenable for examination of mitosis and cytokinesis, as the early embryonic cells are large and the spindle and chromosomes are cytologically observable. Moreover, RNA-mediated interference (RNAi) provides an efficient reverse genetic technique to

eliminate both maternal and zygotic gene functions.[22] Consequently, single, double and triple gene knockdown by RNAi may reveal specific as well as redundant gene functions in early embryogenesis.

The *C. elegans* genome harbors orthologs of all major classes of metazoan cyclins: D, E, A, B1, B2 and B3.[23–28] We show that CYB-1 (Cyclin B1) and CYB-3 (Cyclin B3) follow similar developmental expression patterns and largely overlapping subcellular localizations, yet each of these cyclins is essential for specific processes in meiosis and mitosis. Simultaneous inhibition of *cyb-1* and *cyb-3* results in an earlier and more severe M phase arrest. However, only the combination of *cyb-1*, *cyb-2.1/2.2* and *cyb-3* RNAi resembles *cdk-1* inactivation. These data indicate that all B/B3-type cyclins act with CDK-1 and provide overlapping as well as specific functions in meiosis and mitosis. Our results suggest that phosphorylation of some mitotic Cdk targets can be accomplished by a variety of Cdk1/mitotic cyclin complexes, while phosphorylation of other targets requires a specific Cdk1/cyclin combination.

Results

Caenorhabditis elegans contains distinct subfamilies of mitotic cyclins

Previous studies by us and others identified the *Caenorhabditis elegans* cyclin genes *cyd-1* (Cyclin D),[24,26] *cye-1* (Cyclin E),[25,28] *cya-1* (Cyclin A), *cyb-1* (Cyclin B1) and *cyb-3* (Cyclin B3).[23] The *C. elegans* Genome Sequencing project identified two additional B-type cyclins,[29] encoded by the Y43E12A.1 (*cyb-2.1*) and H31G24.4 (*cyb-2.2*) genes (Fig. 1). We obtained cDNA clones from *cyb-2.1* and *cyb-2.2,* demonstrating that both genes are expressed (Fig. 1A, Materials and Methods). These cDNAs are probably derived from the full-length messages, as they contained SL1 trans-spliced leader sequences at their 5′-ends.[30] The predicted amino-terminal ends of all five *C. elegans* A, B and B3-type cyclins include candidate destruction boxes (Fig. 1A and reviewed in ref. 23). This amino acid motif is present in the N-termini of mitotic cyclins in other systems and is required for ubiquitin-dependent proteolysis.[31]

The *cyb-2.1* and *cyb-2.2* coding sequences share 92% nucleotide identity, indicating a relatively recent duplication. The CYB-2.1 and CYB-2.2 predicted proteins share 94% aminoacid identity over their entire length. Each of these two cyclins is approximately 60% identical to CYB-1. In contrast, CYB-3 is more closely related to cyclin B3 members in other species than to the other mitotic cyclins in *C. elegans* (Fig. 1B). Similar to the B3 cyclins in other species, CYB-3 contains not only Cyclin B-type signature sequences but also A-type sequences within the cyclin box.[32]

Knockdown of *cyb-1, cyb-2.1, cyb-2.2* or *cyb-3* by RNA interference (RNAi) resulted in early embryonic cell division defects and embryonic lethality (see below). In contrast, upon *cyd-1* and *cya-1* RNAi all offspring developed into sterile larvae, and embryonic lethality was not observed (data not shown). As previously reported, *cye-1(RNAi)* resulted in defects in cell polarity establishment and arrest at the approximately 100-cell stage.[25,26,33]

Because of the close similarity at the DNA level, RNAi for either *cyb-2.1* or *cyb-2.2* is expected to downregulate both genes. In addition, *cyb-2.1/2.2* and *cyb-1* share stretches of approximately 80% nucleotide identity that could also lead to co-inhibition. To examine this possibility, we injected a dsRNA fragment unique for *cyb-1* (nucleotide 11–270 of the open reading frame). This specific *cyb-1* dsRNA fragment also resulted in a highly penetrant embryonic lethality. However, injection of dsRNA corresponding to the most unique 107 nucleotides of the *cyb-2.2* coding region did not cause an apparent phenotype (data not shown). We conclude that at least two different mitotic cyclins, *cyb-1* and *cyb-3,* have

essential functions during embryonic development. For this reason, we focused our analysis on *cyb-1* and *cyb-3*.

CYB-1 and CYB-3 specific antisera recognize active kinase complexes

We generated polyclonal antibodies against the full-length CYB-1 and CYB-3 proteins to examine their expression, Cdk association and subcellular localization. Using total *C. elegans* lysate in western blot experiments, the antisera reacted with proteins of the predicted molecular weight for CYB-1 and CYB-3 (41 kD and 45 kD, respectively, Fig. 2A and B). We examined the effects of *cyb-1* and *cyb-3* RNAi to test the specificity of the antibody reactivity. Animals were soaked in dsRNA and their progeny collected and used in western blotting experiments. RNAi treatment resulted in a significant and specific reduction of the candidate CYB-1 and CYB-3 proteins (Fig. 2A). As expected, control RNAi treatment for the essential mitotic gene *lin-5* did not reduce the reactivity with either cyclin antibody (Fig. 2A; reviewed in ref. 34).

RNAi treatment also eliminated specific antibody staining in immunohistochemical experiments. Immunostaining of *C. elegans* embryos with CYB-1 and CYB-3 antisera showed predominantly pronuclear staining at the time of migration before the first mitosis of the fertilized egg (Fig. 2E). *cyb-1* RNAi strongly reduced reactivity with the anti-CYB-1 sera, while CYB-3 reactivity was unaffected. Likewise, *cyb-3* dsRNA completely eliminated immunoreactivity with anti-CYB-3 antibodies, but not with CYB-1 (Fig. 2E). These results demonstrate the specificity of the affinity-purified antibodies and the specificity of the RNAi. However, co-inhibition of *cyb-2.1*/*2.2* and *cyb-1* was also observed in these experiments. Injection of *cyb-2.1* or *cyb-2.2* dsRNA did not affect CYB-3 reactivity, but partly reduced CYB-1 staining (data not shown).

CDK-1/NCC-1 is the *C. elegans* cyclin-dependent kinase essential for progression through mitosis.[35] Based on results in other eukaryotes, this kinase is expected to act with a number of different mitotic cyclins. CYB-1 and CYB-3 co-immunoprecipitated with the CDK-1 kinase, in contrast to control immunoprecipitations with non-specific antibodies (Fig. 2B). In addition, both the CYB-1 and CYB-3 immunoprecipitates demonstrated kinase activity in vitro towards the canonical CDK substrate histone H1 (Fig. 2C; reviewed in ref. 36). These results are consistent with the hypothesis that CYB-1 and CYB-3 act to promote progression through mitosis in *C. elegans*.

The CYB-1 and CYB-3 proteins show largely overlapping expression patterns

To examine whether CYB-1 and CYB-3 showed any marked differences in expression during development, we prepared protein lysates from multiple developmental stages. As expected for mitotic cyclins, the expression levels of CYB-1 and CYB-3 correlated with cell division during each developmental stage (Fig. 2D). The most exponential cell proliferation phase takes place from approximately two through seven hours of embryogenesis. Coincident with expansive proliferation, the highest expression of CYB-1 and CYB-3 proteins was detected in embryos (Fig. 2D, left). CYB-1 and CYB-3 expression was virtually absent in developmentally arrested first stage (Fig. 2D, L1 0 h) and dauer larvae (not shown). Upon release from L1 arrest, sets of post-embryonic blast cells successively initiate cell division,[37] and CYB-1 and CYB-3 levels were found to increase during this period (Fig. 2D, compare: L1 lanes 0 hr and 10 hr). CYB-3 protein levels remained low during larval development, as compared to the levels in embryos, while CYB-1 levels were fairly constant in developing animals.

To examine potential for distinct functions, we studied whether the subcellular localization of CYB-1 and CYB-3 differs. Different subcellular localization has been reported for

vertebrate cyclin B1 and B2,[38] as well as for Drosophila and Chicken cyclin B1 and B3.[32,39] In these systems, cyclin B2 and B3 are restricted to the nucleus, while cyclin B1 accumulates in the cytoplasm during G_2 phase and is rapidly imported into the nucleus at the onset of prophase. Immunostaining of *C. elegans* larvae showed expression of both cyclins in dividing cells (data not shown). However, the strongest expression was detected in the adult germline and early embryos, which we analyzed further.

Precursor germ-cell nuclei are formed in *C. elegans* by mitotic divisions in the distal ends of the syncytial gonad. As these nuclei gradually move further from the distal tip cell, they exit the mitotic cycle, initiate meiosis and go through pachytene of meiotic prophase I. These germ nuclei initiate oocyte development when they reach the bend in the U-shaped gonad; they exit from pachytene, cellularize, continue to enlarge and pause at diakinesis of meiosis I. Meiosis I and II are completed following fertilization, which results in two polar bodies that are expelled from the fertilized egg. Subsequently, a maternal pronucleus forms and migrates towards the paternal pronucleus. The two pronuclei meet in the posterior of the egg, migrate to the middle while rotating and initiate mitosis.

CYB-1 and CYB-3 were detected in the nuclei of the mitotic proliferating region of the gonad (data not shown). During maturation of oocytes in the proximal gonad, CYB-1 and CYB-3 levels were found to gradually increase in the nucleus (data not shown). CYB-1 and CYB-3 remained diffusely distributed throughout the cytoplasm of the fertilized egg during meiosis (Fig. 3A–D), and localized to the maternal and paternal pronuclei upon completion of meiosis (Fig. 3E–H). Subsequently, during each mitotic division, CYB-1 and CYB-3 gradually disappeared from the nucleus as cells proceeded from prophase to metaphase (Fig. 3I–P, posterior cells, to the right). At approximately the time of anaphase initiation, both cyclins also disappeared from the cytoplasm (Fig. 3I–P, anterior cells, to the left). Thus, CYB-1 and CYB-3 show similar temporal and spatial localization. However, CYB-3 localization is mainly nuclear and perdures somewhat longer in metaphase, while a larger fraction of CYB-1 is present in the cytoplasm. These differences are similar, though more subtle, to those reported for cyclin B1 versus B3 localization in other metazoans.[32,38,39]

CYB-1 and CYB-3 have distinct meiotic functions

We used gene inactivation by RNAi to address whether *cyb-1* and *cyb-3* are required for specific cell cycle events in *C. elegans*. Injection of either *cyb-1* or *cyb-3* dsRNA, or the combination of the two, all caused highly penetrant embryonic lethal (Emb) phenotypes. We closely followed early development in *cyb-1(RNAi)* and *cyb-3(RNAi)* embryos as well as double *cyb-1(RNAi); cyb-3(RNAi)* embryos, using microscopic observations of live and fixed specimens (Figs. 4–6). Interestingly, the three different RNAi experiments reproducibly resulted in distinct cell cycle phenotypes, indicating specific cyclin functions.

Neither *cyb-1* nor *cyb-3* RNAi appeared to interfere with events in oogenesis, mature oocytes were formed with chromosomes in typical arrangements of bivalents in diakinesis. Oocytes initiated meiosis normally and became fertilized when entering the spermatheca (not shown). However, meiosis was frequently defective, as was evident from aberrant numbers of polar bodies and maternal pronuclei. In fixed and stained embryos, approximately 56% (43/77) of the *cyb-1(RNAi)* embryos contained just one polar body. Recording of embryogenesis with DIC optics revealed the formation of two maternal pronuclei in 30% (14/46) of *cyb-1(RNAi)* embryos. Of the *cyb-3(RNAi)* embryos, 12% (28/239) did not have any polar bodies and 59% (142/239) contained a single polar body. Embryos examined before the first mitosis formed two maternal pronuclei in 45% (20/44) of the *cyb-3(RNAi)* embryos. Extra pronuclei were always observed in embryos with less than two polar bodies, indicating that failure to dispose of chromosomes within a polar body

resulted in additional pronuclei. Similar observations were made following inactivation of other genes involved in chromosome segregation and cytokinesis.[34,40]

These results indicate that *cyb-1* and *cyb-3* are each required during meiosis. Importantly, time-lapse fluorescence microscopy of meiosis in utero showed that the meiotic defects are distinct. Upon *cyb-1* RNAi, abnormal chromosome alignment and segregation was observed (Fig. 6C, arrow), while *cyb-3* RNAi predominantly caused delayed progression through meiosis II (Fig. 6D, arrow).

CYB-1 is required for chromosome congression, CYB-3 for sister chromatid separation

Regardless of whether two polar bodies were expelled, events immediately following meiosis followed the normal pattern. As in the wild type, the maternal pronucleus migrated towards the paternal pronucleus in the posterior of the egg (Fig. 4B, H and N), the two nuclei migrated to the middle while rotating, the first mitotic spindle was formed and nuclear envelopes disappeared (Fig. 4C, I and O). However, by the time of the metaphase/anaphase transition, mitoses in the *cyb-1(RNAi)* and *cyb-3(RNAi)* embryos diverged from the wild-type and from each other (Fig. 4D, J and P).

When examining wild-type embryos with Nomarski optics, the metaphase-aligned chromosomes are invariably visible during the first mitotic division (Fig. 4C). Chromosome alignment in metaphase is followed immediately by separation of the sister chromatids and migration of sets of chromosomes to the poles during anaphase (Fig. 4D). Coincident with chromosome segregation, the entire DNA/spindle complex migrates with rocking movements to a more posterior position (reviewed in Strome and White).[41] Subsequently, cytokinesis occurs in a plane midway and perpendicular to the spindle, thereby generating two cells of unequal size (Fig. 4E).

The mitotic metaphase plate appeared less well defined in *cyb-1(RNAi)* embryos (Fig. 4I). Segregation of the DNA to opposite poles was initiated without detectable delay; however, the metaphase and anaphase chromosomes continued to be less distinct. By late telophase, multiple nuclei often appeared within a single cell (Fig. 4K and L). To further examine mitotic defects in *cyb-1(RNAi)* embryos, we stained fixed embryos for tubulin and DNA (Fig. 5). The mitotic spindles appeared normal in these embryos and DNA condensation occurred at least partially (Fig. 5B). However, chromosomes often failed to align at the metaphase plate, separated as diffuse masses during anaphase and formed more than two nuclei during telophase. In cells containing multiple nuclei, the amount of DNA in each nucleus varied considerably (data not shown). The mitotic defects observed are not secondary consequences of an abnormal meiosis as similar chromosome congression defects were detected in embryos that completed apparently normal meiosis I and II and extruded two polar bodies (data not shown). These results suggest that *cyb-1* function is required for full condensation and proper congression of the chromosomes at the metaphase plate.

The defects observed in *cyb-3(RNAi)* embryos were clearly distinct from those in *cyb-1(RNAi)* embryos. The formation of pronuclei, pronuclear migration, rotation and bipolar spindle formation all proceeded with some delay (Fig. 4Y), mitosis was initiated and a metaphase plate formed (Fig. 4M–O). However, sister chromatids failed to separate in *cyb-3(RNAi)* embryos (anaphase or telophase figures were not seen in any of the 88 embryos observed). The spindle movements were prolonged and more vigorous, apparently attempting to separate the DNA. Exit from mitosis was significantly delayed in these defective embryos (anaphase onset: 21.75 ± 1.40 vs. 13.22 ± 0.79 min in wild type). Cytokinesis was initiated in the absence of chromosome segregation in all embryos, but the cleavage furrow regressed upon unsuccessful cleavage in the majority of the embryos (Fig. 4P and Q). Duplication and separation of the centrosomes continued, giving rise to

multipolar spindles (Figs. 4Q and 5C). Following abortive mitosis, DNA replication eventually continued and *cyb-3(RNAi)* embryos usually arrested with a single polyploid DNA mass and multiple centrosomes. Again, indistinguishable mitotic defects were observed in embryos that did or did not complete meiosis, indicating that these defects are not secondary consequences of an abnormal meiosis. The absence of sister chromatid separation following *cyb-3* RNAi clearly indicates requirement of *cyb-3* in this process.

In summary, RNAi of *cyb-1* as well as *cyb-3* results in embryonic lethality due to failure of a fundamental aspect of chromosome segregation. Because both cyclins are essential and because their loss-of-function affects different aspects of mitosis, we conclude that CYB-1 and CYB-3 exert distinct mitotic functions.

CYB-1 and CYB-3 also have redundant functions

While RNA interference of *cyb-1* and *cyb-3* each produced a distinct mitotic defect, neither of these defects was as severe or as early as those caused by loss of CDK-1. In *cdk-1(RNAi)* embryos, meiotic chromosome segregation was completely absent, paternal and maternal pronuclei were formed but migrated slowly and the embryos entered a stable arrest upon meeting of the pronuclei and prior to nuclear envelope breakdown.[35] We inactivated both *cyb-1* and *cyb-3* simultaneously to examine whether these genes act redundantly in meiosis and the initial mitotic events (Fig. 4S–X). Although meiosis was defective in the *cyb-1(RNAi); cyb-3(RNAi)* embryos nearly all of the embryos (131/134) expelled a single polar body. Pronuclear migration was severely delayed, requiring up to three times the time of migration in the wild-type embryo, and many embryos did not complete rotation of the joined pronuclei. All embryos arrested prior to the first division upon meeting of the pronuclei (Figs. 4X and Y; 5D). Most embryos contained multiple spindle asters but bipolar spindles were not formed. In approximately half of the embryos (15/33) the paternal pronucleus failed to decondense. In a substantial fraction of the embryos (17/103) the paternal pronucleus migrated to meet with the maternal pronucleus in the anterior of the embryo, opposite of wild-type migration. The fact that *cyb-1 cyb-3* double RNAi results in more severe and earlier defects than either single RNAi indicates that these cyclins have overlapping functions in addition to the specific roles described above.

All mitotic defects observed in the *cyb-1 cyb-3* double RNAi embryos were also seen in *cdk-1(RNAi)* embryos.[35] However, upon *cyb-1 cyb-3* double RNAi meiosis I was still completed (Fig. 6E), in contrast to *cdk-1(RNAi)* embryos (Fig. 6B). This might indicate that CDK-1 functions with yet other cyclins during the first meiotic division. The defects observed in *cyb-2.1/cyb-2.2(RNAi)* embryos resembled those in *cyb-1(RNAi)* embryos (data not shown). As described above, we cannot exclude that the *cyb-2.1/cyb-2.2* phenotype results from co-inhibition of *cyb-1*. However, RNAi for *cyb-2.1/cyb-2.2* further increased the severity of the *cyb-1; cyb-3* RNAi phenotype. Knockdown of all four mitotic cyclins fully phenocopied the *cdk-1(RNAi)* phenotype: the condensed chromosomes remained in typical diakinesis arrangement after fertilization and a meiotic spindle failed to form (Fig. 6F). Exit from meiosis occurred with normal timing (formation of a maternal pronucleus 28 min. post fertilization). The maternal pronucleus migrated slowly towards the posterior and met with the paternal pronucleus, after which the fertilized egg remained stably arrested. We conclude that the different B and B3 cyclins act in part redundantly in meiotic and mitotic M phase, in addition to unique cyclin B versus cyclin B3 functions.

Discussion

All eukaryotes express a series of cyclins that are positive regulators of cell division and likely are derived from a single ancestor.[1,2] Specific cyclins accumulate during different phases of the cell cycle, and thus they can activate CDK partners at different times. Some

cyclins show specificity for distinct CDKs, which allows them to act in specific processes. However, it is less clear if and how different cyclins target the same CDK to different substrates. Although several in vitro studies have indicated substrate specificity for distinct cyclin-CDK complexes, data from in vivo studies are limited, in particular for mitotic cyclins.

Here we show that the *C. elegans* mitotic cyclins CYB-1 and CYB-3 are present in dividing cells at overlapping subcellular locations and with similar cell cycle profiles, and that both cyclins form active complexes with the CDK-1 catalytic subunit. Despite these similarities, each single cyclin is essential and their inactivation results in specific mitotic defects. Loss of *cyb-1* function leads to defects in alignment of the chromosomes at the metaphase plate, while inactivation of *cyb-3* prevents segregation of sister chromatids. Mitosis is prevented altogether when both cyclins are inactivated simultaneously, resembling the mitotic, but not meiotic, *cdk-1(RNAi)* phenotype. Together, these results demonstrate that *C. elegans* cyclins CYB-1 and CYB-3 act in the regulation of mitosis, with overlapping functions in promoting initiation of mitosis and distinct roles in the execution of the chromosome segregation process.

Whether cyclins CYB-2.1 and CYB-2.2 have distinct contributions in mitosis is currently uncertain. Injection of dsRNA corresponding to a small unique fragment of *cyb-2.1*/*2.2* did not cause any apparent abnormalities. Injection of a large dsRNA fragment caused defects similar to *cyb-1* RNAi, but this also reduced CYB-1 levels. While uncertain for mitosis, *cyb-2.1*/*2.2* clearly contribute to meiosis. Meiotic chromosome segregation was entirely blocked only when *cyb-2.1*/*2.2* RNAi was combined with *cyb-1* and *cyb-3* RNAi. Thus, CYB-2.1/2.2 can drive partial progression through meiosis in the absence of CYB-1 and CYB-3, but it cannot do so during the subsequent mitotic division.

A specific function in cell cycle progression may have been expected, at the least for cyclin B3. Cyclin B3 contains sequence motifs of both A- and B-type cyclins and is considered a distinct subfamily of mitotic cyclins, although slightly more closely related to the B subfamily.[32] B3 cyclins are conserved from *C. elegans* to mammals and, in contrast to other cyclins, are encoded by single genes.[27] In any given species, B3 cyclins are more closely related to B3 cyclins in other metazoans than to A- and B-type cyclins within the same species (Fig. 1B). The selective pressure for conservation of a distinct B3 cyclin throughout metazoan evolution may be expected to indicate some functional specificity.

On the other hand, the initial characterization of cyclin B3 in Drosophila revealed predominantly overlapping functions with cyclin B. Paradoxically, the Drosophila cyclins appear to behave more dissimilarly than their *C. elegans* counterparts. Accumulation and destruction of Cyclin B3 in Drosophila succeeds that of cyclin A and cyclin B.[39] In contrast, CYB-1 and CYB-3 seemed present during the same part of the cell cycle and both disappeared very close to the onset of chromosome segregation. Drosophila cyclin B3 is exclusively nuclear, in contrast to cyclin A and B, which accumulate in the cytoplasm and translocate to the nucleus.[6] *C. elegans* CYB-3 is also mainly or exclusively nuclear, while substantial levels of CYB-1 are present in the cytoplasm. However, we have not observed cell cycle dependence in the nuclear translocation of CYB-1. Expression of truncated Drosophila cyclins lacking the destruction box motif also affected mitotic progression in specific ways: Δcyclin A caused metaphase delay, Δcyclin B early anaphase arrest and Δcyclin B3 late anaphase arrest.[39] We have been unable to arrest mitosis in *C. elegans* by expression of truncated cyclins, possibly because the required expression levels were not reached.

A recent study addressed the cyclin contribution to rapid syncytial divisions of Drosophila embryos,[16,42] based on injection of dsRNA and time-lapse fluorescence microscopy. At this time of development, the functional similarities between Drosophila CycB and *C. elegans* CYB-1, as well as Drosophila CycB3 and *C. elegans* CYB-3 are striking. Knockdown of only CycB interfered with chromosome congression in metaphase, while CycB3 depletion disrupted the transition to anaphase. A critical difference is the contribution of cyclin A: while CycA is a major mitotic cyclin in Drosophila, we did not detect a role for its closest *C. elegans* homolog, CYA-1, in embryonic divisions. The Drosophila studies by Jacobs et al.[6] and McCleland et al.[42,43] demonstrate that the maternal contribution of CycB and CycB3 is more critical than their zygotic functions. We focused our analysis on the contribution of B and B3-type cyclins in meiosis and the first embryonic divisions, which require maternal functions. Although beyond the scope of this study, cyclin knockdown through soaking RNAi of first stage larvae and examination of deletion mutants showed that *cyb-3* and, to a lesser extent, *cyb-1* are also essential for progression through mitosis during larval development (data not shown).

If their temporal and spatial expression is similar, what is the critical difference between CYB-1 and CYB-3? Cyclins positively regulate CDKs by changing their conformation to an active state and by contributing to the docking of substrates. The crystal structures of several CDK complexes have provided insights into these cyclin roles.[44] Studies of the cyclin A/Cdk2 structure have shown that cyclin binding changes the position of the so-called T loop in the CDK, so that it no longer blocks access to the catalytic cleft. In addition, upon binding to cyclin, the CDK α-helix that includes the conserved PSTAIRE domain changes position, so that a critical glutamic acid in this domain can contribute to coordinating the phosphate atoms of Mg^{2+}ATP.[44,45]

These roles in CDK activation are thought to be universal and are most likely accomplished by CYB-1 as well as CYB-3. However, specificity may be provided at the level of substrate interaction. The crystal structure of a cyclin A/Cdk2/$p27^{Kip1}$ complex has revealed contact sites between cyclin A and $p27^{Kip1}$.[46] A hydrophobic patch on the cyclin A surface contacts residues of the RXL motif present in these substrates, which is essential for phosphorylation of RXL-containing substrates but not for histone H1 phosphorylation.[18] The hydrophobic pocket contains the MRAIL sequence and is conserved in CYB-1: including the critical residues M143, L147, W150, Q188 and L189 (Marked in Fig. 1A by asterisks). Surprisingly, two of the most critical hydrophobic residues, M143 and L189, are changed to hydrophilic residues T and K, respectively, in CYB-3 (Fig. 1A). Although additional domains may be involved, these differences between CYB-1 and CYB-3 probably affect substrate specificity, as they concern the only substrate-docking site in cyclins known to date.[47]

A compelling question remains as to what specific substrates are phosphorylated by the CYB-1 and CYB-3/CDK-1 kinases. The loss-of-function phenotypes of these cyclins evoke some interesting candidates. The *cyb-1(RNAi)* phenotype is consistent with partially penetrant defects in chromosome condensation and/or microtubule-kinetochore attachments. A number of critical proteins have been identified in these processes (e.g., Desai et al.).[48] However, the fact that most cell divisions complete successfully in *cyb-1(RNAi)* embryos indicates that the actual defects could be subtle. In contrast, lack of sister-chromosome separation in *cyb-3(RNAi)* embryos is a specific and fully penetrant defect. Most mitotic processes in these embryos either occur normally or fail subsequent to chromosome-separation failure. For chromosome segregation to occur, cohesin molecules that hold sister chromatids together need to be degraded. This process involves several sequential steps: activation of the anaphase-promoting complex (APC) leads to degradation of Securin, which allows the protease Separase to become active and to cleave the Scc1 Cohesin subunits.

Phosphorylation by a CYB-3/CDK-1 kinase could regulate any step in this process. Interestingly, in yeast, Cdc28-dependent phosphorylation of APC components is required specifically to promote the Cdc20-dependent (anaphase promoting) activity of the APC, and not for its G_1 activity.[49] Future studies may reveal whether this function is exerted specifically by CYB-3/CDK-1 in *C. elegans*.

Materials and Methods

Culture conditions and strains

C. elegans strains were cultured using standard techniques as described by Brenner[50] and were derived from the wild-type Bristol N2 strain. Strain SV1010 was used for live-imaging (*ruIs57[unc-119*(+) *pie-1*-GFP-α-tubulin*]; itIs37[unc-119*(+) *pie-1*-mCherry-H2B] (may contain unc-119 (eds) III)).

Isolation of cyb-2.1 and cyb-2.2 cDNAs

The genomic and cDNA sequences of *cyb-1* and *cyb-3* were previously reported.[23] The *C. elegans* genome project revealed two additional B-type cyclin genes: Y43E12A.1/*cyb-2.1* located 0.1 map units to the right of *cyb-1* (+4.78, chromosome IV), and H31G24.4/*cyb-2.2* located at −1.65 mu on chromosome I. A 1.5 kb *cyb-2.1* cDNA was kindly provided by Yuji Kohara (National Institute of Genetics, Mishima, Japan). DNA sequence analysis confirmed the open reading frame as predicted by GENEFINDER. A partial cDNA from *cyb-2.2/* H31G24.4 was obtained by reverse transcriptase/PCR amplification. Briefly, 1 μg of poly(A)$^+$ RNA from mixed stage animals was primed using 1 nmol/μl random hexamer primers and copy DNA synthesized with reverse transcriptase. The cDNA was used in standard PCR amplification reactions, cloned into pBSK and examined by DNA sequence analysis.

Antibody production

Full-length *cyb-3* and *cyb-1* cDNAs were cloned into the pET19b expression vector (Novagen) and expressed in *E. coli*. The purified His-tagged CYB-1 and CYB-3 proteins were injected into mice and rabbits according to standard procedures.[51] The specificity of the polyclonal antisera obtained was further improved by adsorption to bacterial proteins and affinity purification. The anti-CYB-1 serum initially contained antibodies recognizing a centrosomal protein, which were removed during the purification.

Western blot analysis and immunohistochemistry

C. elegans protein extract was obtained from developmentally staged wild-type animals. Protein samples were separated on a 10% polyacrylamide gel using SDS-PAGE and the protein was immunoblotted using standard procedures.[51] Mouse monoclonal anti-α-Tubulin antibodies N356 and DM1A (1:3,000, Sigma) were used as loading controls.

Immunostaining of *C. elegans* embryos was as described.[35] Antibodies used for these studies are listed with their respective dilutions: mouse monoclonal anti-α-Tubulin DM1A (1:100; Sigma), mouse polyclonal anti-CYB-3 (1:20), rabbit polyclonal anti-CYB-3 (1:200), rabbit polyclonal anti-CYB-1 (1:20), rabbit polyclonal anti-CDK-1/NCC-1 1755 (1:100). Secondary FITC- or Texas Red-conjugated antibodies were used at 1:100 dilutions (Jackson ImmunoResearch Laboratories). DNA was stained with 1 μg/ml 4,6-diamidino-2-phenylindole (DAPI; Sigma). Samples were mounted on slides in Prolong Antifade Gold.

Immunoprecipitation and H1 kinase assays

Lysates for immunoprecipitations were obtained from *C. elegans* embryos, lysed and sonicated in lysis buffer (10 mM HEPES pH 7.4, 0.5 mM EDTA, 2.5 mM EGTA, 2.5 mM $MgSO_4$, 15% glycerol, 250 mM NaCl, 0.5% Triton X-100, 1 μg/ml aprotinin, 1 μg/ml leupeptin, 1 μg/ml trypsin inhibitor, 1 mM NaF and 2 mM PMSF). CYB-1, CYB-3 and CDK-1 were immunoprecipitated from embryonic lysates containing 500 μg total protein, using 20 μl Protein A beads cross-linked to antibody. The beads were washed 4X in lysis buffer. Half of the beads were boiled in 2X sample buffer, followed by SDS-PAGE, western blotting and probing with the anti-PSTAIRE monoclonal antibody (1:2,000 dilution). The remaining beads were washed 2X in kinase buffer (50 mM HEPES pH 7.4, 25 mM $MgCl_2$, 5 mM DTT) and incubated in a 50 μl reaction mix containing kinase buffer, 1 μg histone H1 (Gibco) and 5 μCi [γ-^{32} P]ATP for 30 minutes at 30°C. The beads were boiled in 2X sample buffer and the supernatant was run on a 12% SDS polyacrylamide gel. Preimmune rabbit serum was used as a negative control.

Isolation of synchronized developmental stages

To obtain protein samples representing the developmental stages of the worm, synchronized *C. elegans* wild-type animals were isolated from eggs, larval stages 1–4, adults, gravid adults and developmentally-arrested dauer larvae. Eggs were obtained by hypochlorite treatment of gravid adults. For L1 arrested animals, eggs were hatched in M9 in the absence of food for 24 hours and then harvested. For L1, L2, L3, L4, adult and gravid adult animals, embryos were hatched in the presence of food and incubated at 20°C for 10, 20, 29, 39, 52 and 70 hrs., respectively, and then harvested. All stages were analyzed by microscopy before harvesting to ensure proper development. For protein lysate, animals staged above were collected, an equal volume of 2X Laemmli buffer was added and proteins were released by boiling for 5 minutes.

RNA interference

Plasmids used for in vitro transcription contained full-length *cyb-1*, *cyb-2.1, cyb-2.2, cyb-3* or *lin-5* cDNA, a 260 bp *cyd-1* fragment, corresponding to nucleotides 11–270 of the open reading frame (ORF), or a 107 bp fragment of *cyb-2.2*, corresponding to nucleotides 53–160 of the ORF. Templates were linearized and transcribed using T3 or T7 polymerase (Ambion). RNA was phenol extracted, ethanol precipitated and dissolved in 1X injection buffer (20% polyethylene glycol 8000, 200 mM KPO_4 pH 7.5, 30 mM KCitrate pH 7.5) to a final concentration of ~1 mg/ml. The antisense and sense transcripts were annealed and injected into early adult N2 hermaphrodites as described by Fire et al.[22] Injected wild-type animals were singled onto plates and transferred every 12 hours to score the entire brood. For western blot analysis, synchronized L4 larvae were soaked in a *cyb-1* or *cyb-3* dsRNA solution for 24 hours at 20°C, transferred to a plate with food to accumulate eggs, followed by hypochlorite treatment to harvest embryos. For larval RNAi, L1 animals synchronized in the absence of food were incubated in *cyb-1* or *cyb-3* dsRNA solution for 24 hours before placing them on plates with food.

Nomarski observations and recordings

Meiotic divisions were followed in utero after anesthetization of adult worms with 0.1% tricaine and 0.01% tetramisole on 2% agarose pads. Early embryonic events were recorded using time-lapse video microscopy typically from pronuclear formation to the four-cell stage (one image every 10 seconds). Embryos from either wild-type or dsRNA-injected hermaphrodites were dissected and mounted onto agarose pads as described.[52]

Microscopy and image acquisition

A Zeiss Axioplan II microscope was used for Nomarski and immunofluorescence microscopy. Cell divisions were recorded with a 100x 1.4 numerical aperture PlanApochromat objective lens on a motorized microscope (Zeiss Axioplan). Meiotic divisions were recorded with a 30-sec interval with 400 ms fluorescent exposure. Fluorescent excitation light was filtered to 10% transmission with neutral density filters, and binning was set to 2 × 2 with automatic gain adjustments. Microinjections were performed using a Nikon inverted microscope and Narishige micromanipulator.

Acknowledgments

We thank Andy Golden for CDK-1/NCC-1 specific antibodies, Masakane Yamashita for anti-PSTAIRE antibodies, and Yuji Kohara for *cyb-2.1* cDNA. We acknowledge Mike Boxem for critically reading the manuscript. This work was supported by the NIH, RO1 GM057990 to S.v.d.H., by a postdoctoral fellowship from the Medical Foundation to M.A.L., and by a William Starr Fellowship to D.G.S.

References

1. Morgan DO. Cyclin-dependent kinases: engines, clocks and microprocessors. Annu Rev Cell Dev Biol. 1997; 13:261–91. [PubMed: 9442875]
2. Satyanarayana A, Kaldis P. Mammalian cell cycle regulation: several Cdks, numerous cyclins and diverse compensatory mechanisms. Oncogene. 2009; 28:2925–39. [PubMed: 19561645]
3. Sherr CJ. Cancer cell cycles. Science. 1996; 274:1672–7. [PubMed: 8939849]
4. Fitch I, Dahmann C, Surana U, Amon A, Nasmyth K, Goetsch L, et al. Characterization of four B-type cyclin genes of the budding yeast *Saccharomyces cerevisiae*. Mol Biol Cell. 1992; 3:805–18. [PubMed: 1387566]
5. Richardson H, Lew DJ, Henze M, Sugimoto K, Reed SI. Cyclin-B homologs in *Saccharomyces cerevisiae* function in S phase and in G_2. Genes Dev. 1992; 6:2021–34. [PubMed: 1427070]
6. Jacobs HW, Knoblich JA, Lehner CF. Drosophila Cyclin B3 is required for female fertility and is dispensable for mitosis like Cyclin B. Genes Dev. 1998; 12:3741–51. [PubMed: 9851980]
7. Murphy M, Stinnakre MG, Senamaud-Beaufort C, Winston NJ, Sweeney C, Kubelka M, et al. Delayed early embryonic lethality following disruption of the murine cyclin A2 gene. Nat Genet. 1997; 15:83–6. [PubMed: 8988174]
8. Brandeis M, Rosewell I, Carrington M, Crompton T, Jacobs MA, Kirk J, et al. Cyclin B2-null mice develop normally and are fertile whereas cyclin B1-null mice die in utero. Proc Natl Acad Sci USA. 1998; 95:4344–9. [PubMed: 9539739]
9. Fantl V, Stamp G, Andrews A, Rosewell I, Dickson C. Mice lacking cyclin D1 are small and show defects in eye and mammary gland development. Genes Dev. 1995; 9:2364–72. [PubMed: 7557388]
10. Sicinski P, Donaher JL, Parker SB, Li T, Fazeli A, Gardner H, et al. Cyclin D1 provides a link between development and oncogenesis in the retina and breast. Cell. 1995; 82:621–30. [PubMed: 7664341]
11. Sicinski P, Donaher JL, Geng Y, Parker SB, Gardner H, Park MY, et al. Cyclin D2 is an FSH-responsive gene involved in gonadal cell proliferation and oncogenesis. Nature. 1996; 384:470–4. [PubMed: 8945475]
12. Sicinska E, Aifantis I, Le Cam L, Swat W, Borowski C, Yu Q, et al. Requirement for cyclin D3 in lymphocyte development and T cell leukemias. Cancer Cell. 2003; 4:451–61. [PubMed: 14706337]
13. Geng Y, Whoriskey W, Park MY, Bronson RT, Medema RH, Li T, et al. Rescue of cyclin D1 deficiency by knockin cyclin E. Cell. 1999; 97:767–77. [PubMed: 10380928]
14. Carthon BC, Neumann CA, Das M, Pawlyk B, Li T, Geng Y, et al. Genetic replacement of cyclin D1 function in mouse development by cyclin D2. Mol Cell Biol. 2005; 25:1081–8. [PubMed: 15657434]
15. Santamaria D, Barriere C, Cerqueira A, Hunt S, Tardy C, Newton K, et al. Cdk1 is sufficient to drive the mammalian cell cycle. Nature. 2007; 448:811–5. [PubMed: 17700700]

16. McCleland ML, Farrell JA, O'Farrell PH. Influence of cyclin type and dose on mitotic entry and progression in the early Drosophila embryo. J Cell Biol. 2009; 184:639–46. [PubMed: 19273612]
17. Moore JD, Kirk JA, Hunt T. Unmasking the S-phase-promoting potential of cyclin B1. Science. 2003; 300:987–90. [PubMed: 12738867]
18. Schulman BA, Lindstrom DL, Harlow E. Substrate recruitment to cyclin-dependent kinase 2 by a multipurpose docking site on cyclin A. Proc Natl Acad Sci USA. 1998; 95:10453–8. [PubMed: 9724724]
19. Loog M, Morgan DO. Cyclin specificity in the phosphorylation of cyclin-dependent kinase substrates. Nature. 2005; 434:104–8. [PubMed: 15744308]
20. Cross FR, Yuste-Rojas M, Gray S, Jacobson MD. Specialization and targeting of B-type cyclins. Mol Cell. 1999; 4:11–9. [PubMed: 10445023]
21. Peeper DS, Parker LL, Ewen ME, Toebes M, Hall FL, Xu M, et al. A- and B-type cyclins differentially modulate substrate specificity of cyclin-cdk complexes. EMBO J. 1993; 12:1947–54. [PubMed: 8491188]
22. Fire A, Xu S, Montgomery MK, Kostas SA, Driver SE, Mello CC. Potent and specific genetic interference by double-stranded RNA in *Caenorhabditis elegans*. Nature. 1998; 391:806–11. [PubMed: 9486653]
23. Kreutzer MA, Richards JP, De Silva-Udawatta MN, Temenak JJ, Knoblich JA, Lehner CF, et al. *Caenorhabditis elegans* cyclin A- and B-type genes: a cyclin A multigene family, an ancestral cyclin B3 and differential germline expression. J Cell Sci. 1995; 108:2415–24. [PubMed: 7545687]
24. Park M, Krause MW. Regulation of postembryonic G_1 cell cycle progression in *Caenorhabditis elegans* by a cyclin D/CDK-like complex. Development. 1999; 126:4849–60. [PubMed: 10518501]
25. Fay DS, Han M. Mutations in *cye-1*, a *Caenorhabditis elegans* cyclin E homolog, reveal coordination between cell cycle control and vulval development. Development. 2000; 127:4049–60. [PubMed: 10952902]
26. Boxem M, van den Heuvel S. lin-35 Rb and cki-1 Cip/Kip cooperate in developmental regulation of G_1 progression in *C. elegans*. Development. 2001; 128:4349–59. [PubMed: 11684669]
27. Nieduszynski CA, Murray J, Carrington M. Whole-genome analysis of animal A- and B-type cyclins. Genome Biol. 2002:3.
28. Brodigan TM, Liu J, Park M, Kipreos ET, Krause M. Cyclin E expression during development in *Caenorhabditis elegans*. Dev Biol. 2003; 254:102–15. [PubMed: 12606285]
29. Science. 1998; 282:2012–8. [PubMed: 9851916]
30. Krause M, Hirsh D. A trans-spliced leader sequence on actin mRNA in *C. elegans*. Cell. 1987; 49:753–61. [PubMed: 3581169]
31. King RW, Peters JM, Tugendreich S, Rolfe M, Hieter P, Kirschner MW. A 20S complex containing CDC27 and CDC16 catalyzes the mitosis-specific conjugation of ubiquitin to cyclin B. Cell. 1995; 81:279–88. [PubMed: 7736580]
32. Gallant P, Nigg EA. Identification of a novel vertebrate cyclin: cyclin B3 shares properties with both A- and B-type cyclins. EMBO J. 1994; 13:595–605. [PubMed: 8313904]
33. Cowan CR, Hyman AA. Cyclin E-Cdk2 temporally regulates centrosome assembly and establishment of polarity in *Caenorhabditis elegans* embryos. Nat Cell Biol. 2006; 8:1441–7. [PubMed: 17115027]
34. Lorson MA, Horvitz HR, van den Heuvel S. LIN-5 is a novel component of the spindle apparatus required for chromosome segregation and cleavage plane specification in *Caenorhabditis elegans*. J Cell Biol. 2000; 148:73–86. [PubMed: 10629219]
35. Boxem M, Srinivasan DG, van den Heuvel S. The *Caenorhabditis elegans* gene *ncc-1* encodes a *cdc2*-related kinase required for M phase in meiotic and mitotic cell divisions, but not for S phase. Development. 1999; 126:2227–39. [PubMed: 10207147]
36. Shirayama M, Soto MC, Ishidate T, Kim S, Nakamura K, Bei Y, et al. The Conserved Kinases CDK-1, GSK-3, KIN-19, and MBK-2 Promote OMA-1 Destruction to Regulate the Oocyte-to-Embryo Transition in *C. elegans*. Curr Biol. 2006; 16:47–55. [PubMed: 16343905]

37. Sulston JE, Horvitz HR. Post-embryonic cell lineages of the nematode, *Caenorhabditis elegans*. Dev Biol. 1977; 56:110–56. [PubMed: 838129]
38. Jackman M, Firth M, Pines J. Human cyclins B1 and B2 are localized to strikingly different structures: B1 to microtubules, B2 primarily to the Golgi apparatus. EMBO J. 1995; 14:1646–54. [PubMed: 7737117]
39. Sigrist S, Jacobs H, Stratmann R, Lehner CF. Exit from mitosis is regulated by Drosophila *fizzy* and the sequential destruction of cyclins A, B and B3. EMBO J. 1995; 14:4827–38. [PubMed: 7588612]
40. van der Voet M, Berends CW, Perreault A, Nguyen-Ngoc T, Gonczy P, Vidal M, et al. NuMA-related LIN-5, ASPM-1, calmodulin and dynein promote meiotic spindle rotation independently of cortical LIN-5/GPR/Galpha. Nat Cell Biol. 2009; 11:269–77. [PubMed: 19219036]
41. White J, Strome S. Cleavage plane specification in *C. elegans*: how to divide the spoils. Cell. 1996; 84:195–8. [PubMed: 8565065]
42. McCleland ML, O'Farrell PH. RNAi of mitotic cyclins in Drosophila uncouples the nuclear and centrosome cycle. Curr Biol. 2008; 18:245–54. [PubMed: 18291653]
43. Kallio MJ, McCleland ML, Stukenberg PT, Gorbsky GJ. Inhibition of aurora B kinase blocks chromosome segregation, overrides the spindle checkpoint, and perturbs microtubule dynamics in mitosis. Curr Biol. 2002; 12:900–5. [PubMed: 12062053]
44. Jeffrey PD, Russo AA, Polyak K, Gibbs E, Hurwitz J, Massague J, et al. Mechanism of CDK activation revealed by the structure of a cyclinA-CDK2 complex. Nature. 1995; 376:313–20. [PubMed: 7630397]
45. Brown NR, Lowe ED, Petri E, Skamnaki V, Antrobus R, Johnson LN. Cyclin B and cyclin A confer different substrate recognition properties on CDK2. Cell Cycle. 2007; 6:1350–9. [PubMed: 17495531]
46. Russo AA, Jeffrey PD, Patten AK, Massague J, Pavletich NP. Crystal structure of the $p27^{Kip1}$ cyclin-dependent-kinase inhibitor bound to the cyclin A-Cdk2 complex. Nature. 1996; 382:325–31. [PubMed: 8684460]
47. Lee HJ, Chua GH, Krishnan A, Lane DP, Verma CS. Substrate specificity of cyclins determined by electrostatics. Cell Cycle. 2007; 6:2219–26. [PubMed: 17890901]
48. Desai A, Rybina S, Muller-Reichert T, Shevchenko A, Hyman A, Oegema K. KNL-1 directs assembly of the microtubule-binding interface of the kinetochore in *C. elegans*. Genes Dev. 2003; 17:2421–35. [PubMed: 14522947]
49. Rudner AD, Murray AW. Phosphorylation by Cdc28 activates the Cdc20-dependent activity of the anaphase-promoting complex. J Cell Biol. 2000; 149:1377–90. [PubMed: 10871279]
50. Brenner S. The genetics of *Caenorhabditis elegans*. Genetics. 1974; 77:71–94. [PubMed: 4366476]
51. Harlow, E.; Lane, D. Using Antibodies: a laboratory manual. Cold Spring Harbor: Cold Spring Harbor Laboratory press; 1999.
52. Sulston JE, Schierenberg E, White JG, Thomson JN. The embryonic cell lineage of the nematode *Caenorhabditis elegans*. Dev Biol. 1983; 100:64–119. [PubMed: 6684600]

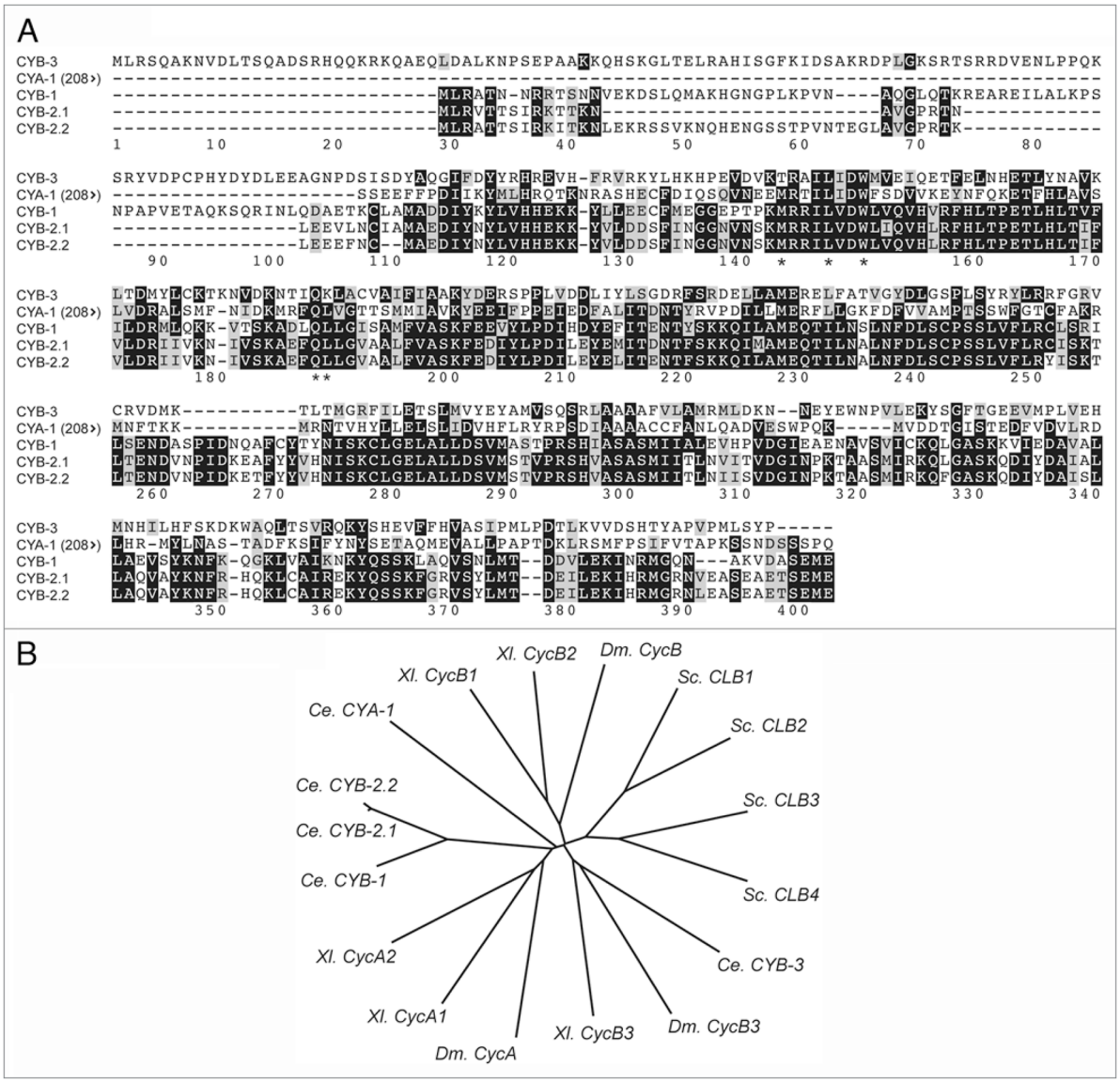

Figure 1.

Distinct mitotic cyclin A, B and B3 genes are conserved in *Caenorhabditis elegans*. (A) Alignment of *C. elegans* CYA-1, CYB-1, CYB-2.1, CYB-2.2 and CYB-3 coding sequences with ClustalW2 and BoxShade. Asterisks (*) indicate predicted residues of the hydrophobic patch involved in substrate docking. Note that Met144 and Leu191 are not conserved in CYB-3 (B) Phylogenetic tree of the predicted A-, B- and B3-type cyclins from *C. elegans (Ce), D. melanogaster (Dm), X. laevis (Xl)* and B-type cyclins of *S. cerevisiae (Sc)* visualized with Phylip DrawTree. Note that the B3-type cyclins are more closely related to cyclin B3 in other species than to other A- and B-type cyclins within the same species.

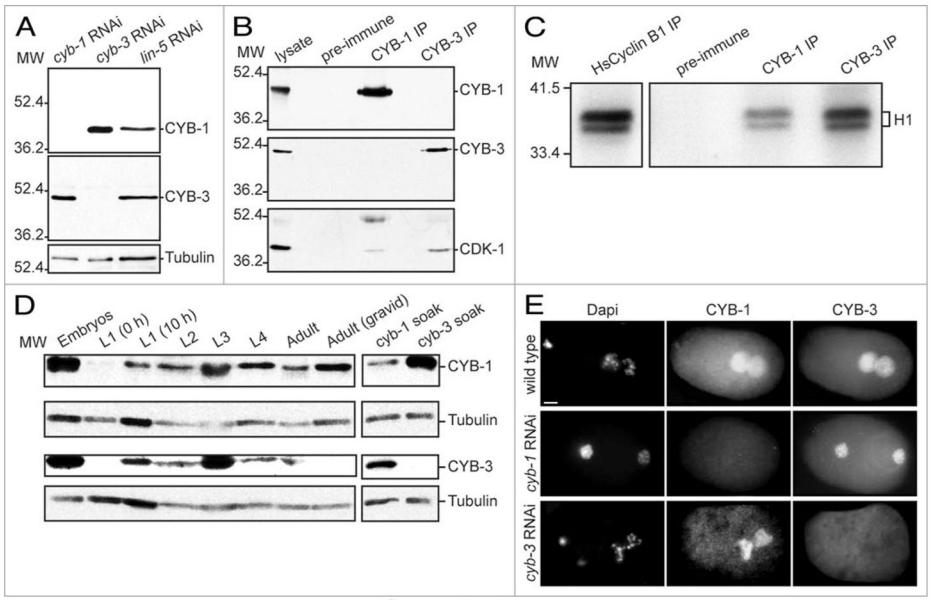

Figure 2.

CYB-1 and CYB-3 bind CDK-1, show associated H1 kinase activity in vitro, and are expressed coincident with cell division. (A) Western blot showing that CYB-1 and CYB-3 antisera are specific. Lanes contain total embryonic protein lysate, obtained after soaking adults in *cyb-1* (left), *cyb-3* (middle) or *lin-5* (right, control) dsRNA. CYB-1 (top), CYB-3 (middle) or anti-α-tubulin antibodies (bottom; loading control) were used for detection. (B) CYB-1 and CYB-3 associate with CDK-1 and (C) form active kinase complexes. Total lysate or immunoprecipitates with the indicated antibodies were used. (D) CYB-1 and CYB-3 protein expression correlate with cell division during development. Protein lysates of synchronized wild-type animals were immunoblotted and probed with the indicated anti-cyclin antibodies. Larval stages are shown. L1 0 hr: developmentally arrested first stage (L1) larvae; L1 10 hr: L1 larvae 10 hr after stimulation of development by food addition. α-Tubulin protein levels serve as a loading control. (E) *cyb-1* and *cyb-3* RNAi specifically reduce expression of the corresponding proteins. Wild-type or RNAi-treated embryos were triple-stained for DNA (DAPI, left), CYB-1 (middle) and CYB-3 (right). Anterior is to the left, scale bar approx. 10 μm.

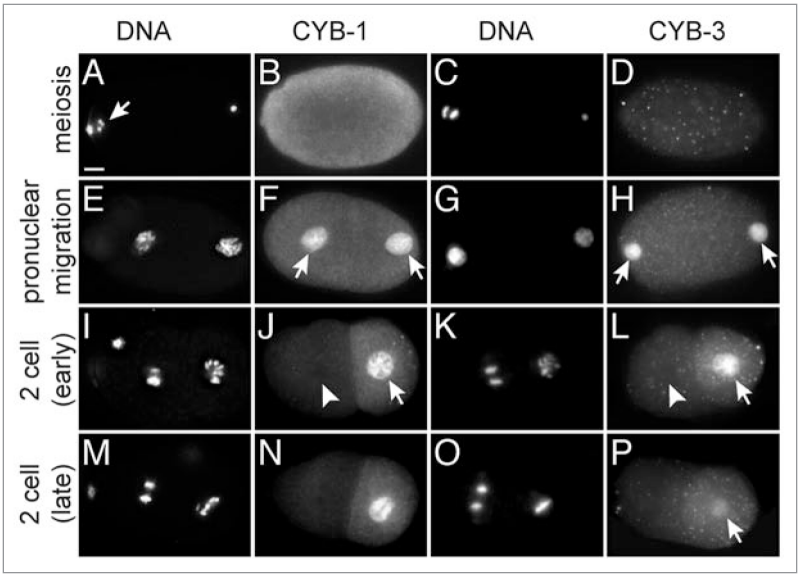

Figure 3.

CYB-1 and CYB-3 show largely overlapping protein localizations. (A and B) CYB-1 and (C and D) CYB-3 localization are cytoplasmic in meiosis. (E–H) Following the completion of meiosis, CYB-1 and CYB-3 localize to the maternal pronucleus in the anterior (left arrow) and paternal pronucleus (right arrow). CYB-1 in particular is also present in the cytoplasm. (I–L) CYB-1 and CYB-3 remain present in the cytoplasm and nucleus during prophase, but are undetectable in anaphase. Two-cell embryos in which the anterior AB cell is in anaphase (arrowhead) and the posterior P1 cell in prophase (arrow). CYB-1 and CYB-3 are present in prophase but not in anaphase. (M–P) Similar but somewhat later embryos, in which P1 is in metaphase. Embryos were stained for DNA (DAPI) and anti-CYB-1 or CYB-3 antibodies. Anterior is to the left, scale bar approx. 10 μm.

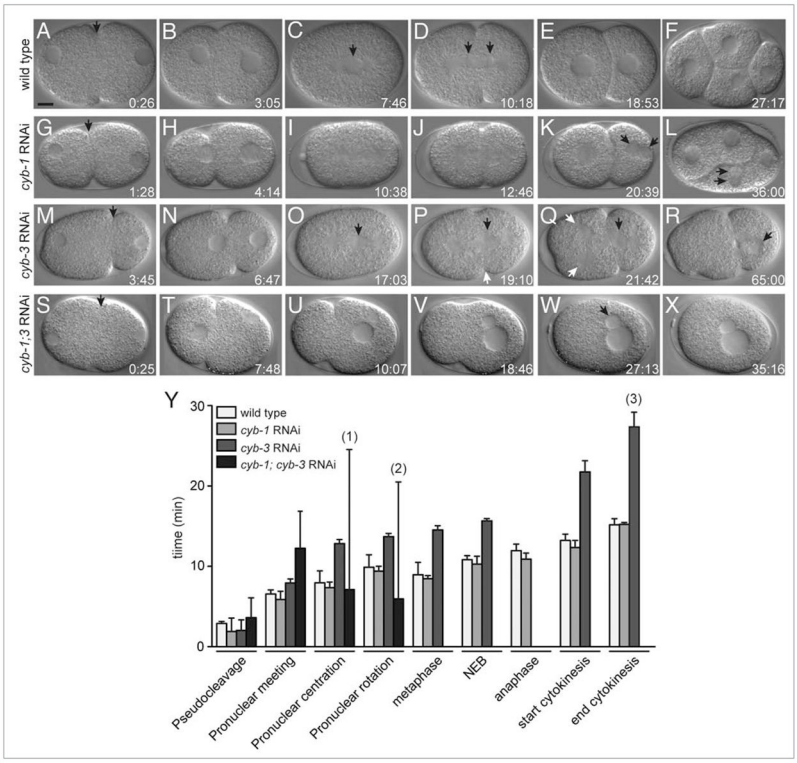

Figure 4.

Mitotic defects associated with CYB-1 and CYB-3 knockdown. (A–F) Development of a wild-type embryo from pronuclear formation until the four-cell stage. The metaphase plate is indicated by a single arrow; segregating chromosomes in anaphase by the double arrows. (G–L) *cyb-1(RNAi)* embryo. Alignment of the chromosomes at the metaphase plate is incomplete; however, chromosome segregation continues, frequently followed by the formation of multiple nuclei within a single cell. Arrows in (K and L) show the formation of multiple nuclei in the posterior P1 cell following the first mitosis and in the EMS cell after division of P1. (C) *cyb-3(RNAi)* embryo. Black arrows point to metaphase-aligned chromosomes, white arrow point to furrow ingression (in P) and spindle poles (in Q). Sister chromatids fail to separate (note the expanded time in the right image). In most embryos, a cleavage furrow forms, fails to complete abscission and subsequently regresses (D) *cyb-1;cyb-3* double RNAi embryo arrests prior to initiation of the first mitosis. A (single) polar body is expelled during meiosis and the pronuclei move together slowly. No further development is observed. Selected images are from time-lapse DIC recordings of living embryos. Scale bar approx. 10 μm. (Y) Timing of events following meiosis, appearance of a maternal pronucleus was taken as $t = 0$. Wild-type (n = 3), *cyb-1* RNAi (n = 3), *cyb-3* RNAi (n = 4), *cyb-1;cyb-3* RNAi (n = 6). (1) 5/6 *cyb-1;cyb-3* RNAi embryos failed pronuclear centration, (2) 5/6 *cyb-1;cyb-3* RNAi embryos failed pronuclear rotation, (3) 1/4 *cyb-3* RNAi embryos failed cytokinesis.

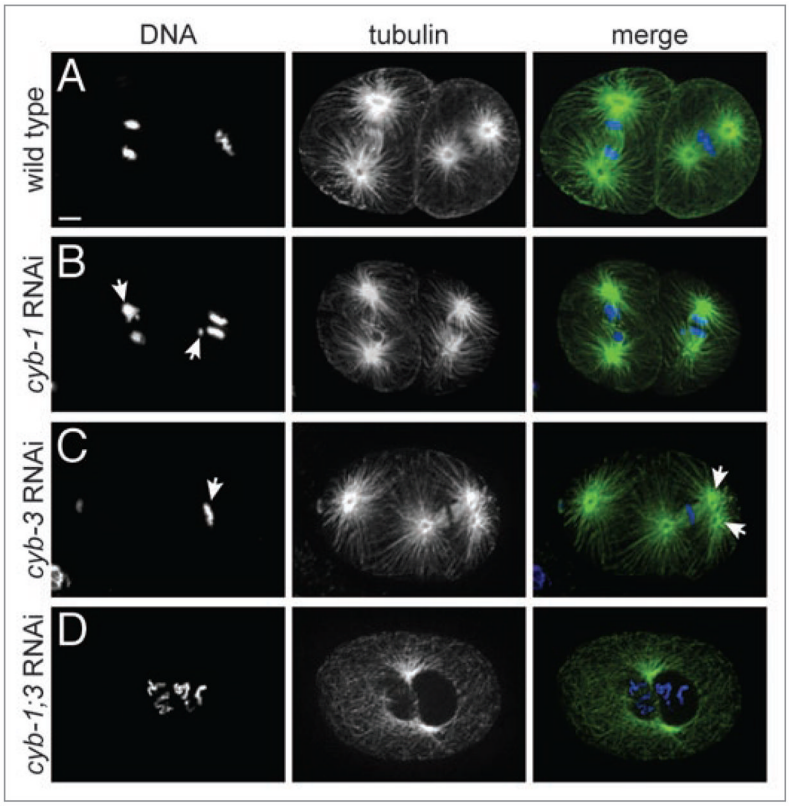

Figure 5.

Distinct mitotic defects in *cyb-1(RNAi), cyb-3(RNAi)* and *cyb-1-;cyb-3* double RNAi embryos. Images show similar stage embryos, double-stained for DNA (left) and α-tubulin (middle). Merged images are to the right. (A) wild-type two-cell embryo, with bipolar spindles and AB cell in anaphase (left) and P1 in metaphase (right). (B) two-cell stage *cyb-1(RNAi)* embryo, arrows indicate unequal DNA segregation in anaphase of AB (see arrow), and a presumed lagging chromosome in metaphase of P1 (right cell, arrow). (C) *cyb-3(RNAi)* embryo demonstrating lack of chromosome segregation, with continued spindle poles duplication. (D) *cyb-1;cyb-3* double RNAi embryo arrested before fusion of the maternal and paternal pronuclei. Anterior is to the left, scale bar 10 μm.

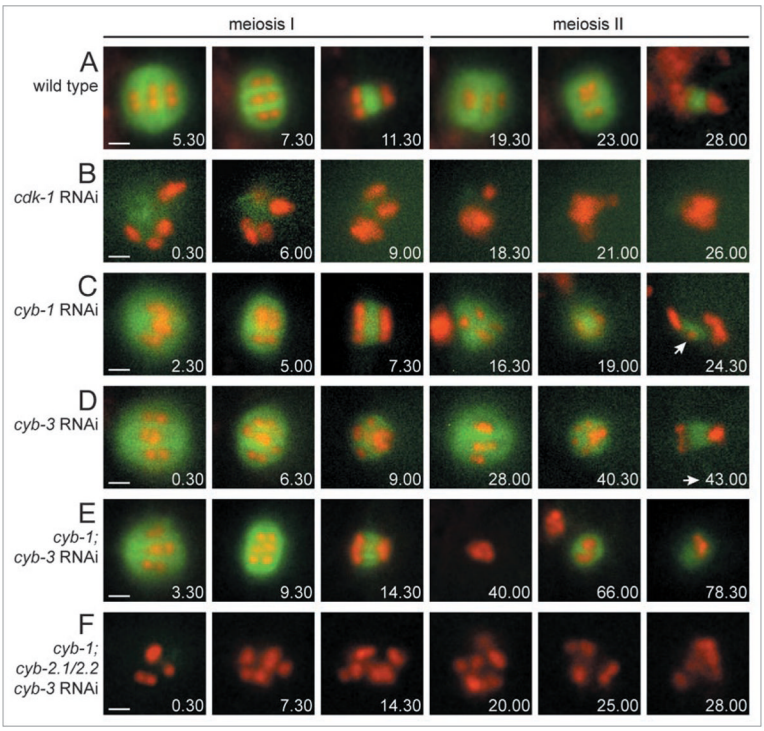

Figure 6.

Time-lapse fluorescent microscopy demonstrates meiotic defects. Images show still-shots of meiotic time-lapse movies in utero. (A) wild-type meiosis I and II; chromosomes align at a metaphase spindle (*t* = 5:30; 19:30), the spindle rotates by 90° (*t* = 7:30; 23:00), and segregates the chromosomes during anaphase (*t* = 11.30; 28.00). (B) RNAi of *cdk-1*. Chromosomes remain in a diakinesis arrangement with limited microtubule organization, the spindle fails to form, but exit from meiosis happens with normal timing. (C) RNAi of *cyb-1* results in meiotic defects in chromosome alignment and segregation (white arrow). (D) RNAi of *cyb-3* results in a substantial delay in metaphase of meiosis II. (E) Double RNAi of *cyb-1* and *cyb-3* results in a dramatic meiosis II defect, while meiosis I is delayed but still completes. (F) Triple RNAi of *cyb-1, cyb-2.1/2.2, cyb-3* results in diakinesis arrest, similar to *cdk-1* RNAi. Red: H2B::Cherry, green: α-tubulin::GFP. Time after entry into the uterus is indicated in each panel. Scale bar is 2 μm, the future anterior cortex is to the left.